ISEIS

Journal of Environmental Informatics 26(1) 14-26 (2015)

Journal of Environmental Informatics

www.iseis.org/jei

Effect of Rainfall Measurement Errors on Nonpoint-Source Pollution Model Uncertainty

Z. Y. Shen*, L. Chen, and Q. Liao

State Key Laboratory of Water Environment Simulation, School of Environment, Beijing Normal University, Beijing 100875, China

Received 8 October 2012; revised 27 April 2013; accepted 17 August 2013; published online 6 August 2015

ABSTRACT. Rainfall data are generally considered the most important input in watershed models and a major source of total uncertainty. This paper investigated the effects of rainfall measurement errors on hydrologic and nonpoint source pollution (H/NPS) modeling in the Daning River watershed in the Three Gorges Reservoir Region (TGRR) of China. The daily rainfall values were randomly permutated by Monte Carlo (MC) sampling, and 150 combinations of rainfall inputs were estimated using the Soil and Water Assessment Tool (SWAT). Based on the results, the rainfall measurement error is transformed into hydrologic modeling uncertainty and further propagates into even larger NPS modeling uncertainty. It was expected from the SWAT applications that the rainfall measurement error would introduce considerable prediction uncertainty especially during high-flow periods. Additionally, the model outputs become more accurate at the expense of a wider 90% confidence interval (90CI) when more possible error values were included. In this case, this paper combined the stochastic modeling and establishing a multi-event uncertainty analysis.

Keywords: rainfall, uncertainty, nonpoint-source pollution, SWAT, Monte Carlo method, Three Gorges Reservoir Region

1. Introduction

Hydrologic and nonpoint-source pollution (H/NPS) models have been developed for practical water resource and quality investigations, as well as subsequent policy-making (Gunalay et al., 2012). However, managers often doubt the reliability of these models because of their associated uncertainties (Beven and Alcock, 2012). Watershed modeling is now described as 'intellectually dishonest' when not accompanived by uncertainty analysis (Hughes, 2010). The errors involved in model input, recognized as a major source of the total uncertainty in model-based Total Maximum Daily Load plan, should be considered, starting from the very beginning.

Rainfall data are generally considered the most important input because rainfall is the major force in runoff production and pollutant transportation (Faurès et al., 1995; Tapiador et al., 2012). Traditionally, a rain gauge is the fundamental measurement tool as the source of precipitation observations as it provides a direct physical record of the precipitation in a given spot (Bárdossy and Das, 2008). In this respect, the accuracy of rainfall data plays a fundamental role in the reliability of watershed models and their application to water quality and risk management (Bohnenstengel et al., 2011; Sun et al., 2012). Many studies have investigated the effect of precipitation input on hydrologic modeling, where the error is propagated from the input data to flow outputs (Gabellani et al., 2007; Schuurmans and Bierkens, 2007; McMillan et al., 2011). It has been speculated that the consideration of spatial rainfall variability is particularly important in both large-scale modeling and small-scale watershed simulations (Osborn et al., 1979; Faures et al., 1995; Cho et al., 2009; Fu et al., 2011). Thus, a well-designed network of rain gauges, in terms of the number of stations and their locations, is crucial to capturing the irregular occurrence, duration and magnitude of rainfall (McMillan et al., 2011; Shen et al., 2012a).

Another uncertainty source is the accuracy of the recorded rainfall data, which provide a direct physical record in a given spot (Renard et al., 2011). Generally, the nature of the rainfall measurement is governed by complicated physical processes, and the recorded values will inevitably deviate from reality (Tapiador et al., 2012). There are two main sources of uncertainty inherent in rainfall measurement: systematic error and random error (Schuurmans and Bierkens, 2007). Systematic error can be defined as distortion due to inadequate positioning, improper calibration, and incorrect installation of equipment (Moulin et al., 2009). Random error is considered as perturbations from the surrounding environment, such those due to the effects of wind and temperature (Seed and Austin, 1990). These errors exist even with the best equipment and correct operation; thus, these errors are reported as inherent parts of the rainfall measurement (Tapiador et al., 2012). It is increasingly recognized that model parameters and structural hypotheses are affected by the quality of the recorded rainfall data (Liu et al., 2009). However, although the impact of rain-

* Corresponding author. Tel.: +86 10 58800398; fax: +86 10 58800398.
E-mail address: zyshen@bnu.edu.cn (Z. Y. Shen).

ISSN: 1726-2135 print/1684-8799 online
 doi:10.3808/jei.201400271

fall measurement error is already a well-researched area of hydrology, there are few studies investigating its effects on NPS simulation.

The Three Gorges Project, situated in Hubei Province, China, is the largest hydropower project in the world. Although the Project has benefits in terms of flood control and power generation, it is also vulnerable to NPS pollution due to excessive human activities (Zhang and Lou, 2011). A number of watershed models have been applied in this region to study the impact of the Project (Shi et al., 2012). However, research concerning the prediction uncertainty in such an important watershed is lacking. The objective of this paper is to contribute an in-depth investigation to ongoing work on rainfall error propagation through the watershed model. The Soil and Water Assessment Tool (SWAT) (Arnold et al., 1998) and Monte Carlo (MC) sampling (Kao and Hong, 1996) were combined to quantify the prediction uncertainty in the Daning River watershed in the Three Gorges Reservoir Region (TGRR) of China.

2. Materials and Methods

2.1. Watershed Description

This study was conducted in the Daning River Watershed, a 2,422 km^2 agricultural watershed (108°44' ~ 110°11'E, 31° 04' ~ 31°44' N) within the central part of the Three Gorges Reservoir Area (TGRA) (Figure 1). The Daning Watershed is dominated by mountains (95%) and low hills (5%), lying at an altitude of 200 to 2588 m and generally decreasing in elevation from northeast to southwest. The land-use includes cropland (22.2%), grassland (11.4%) and forest (65.8%) and the surface soil textures are yellow-brown soil (26.5%), yellow cinnamon soil (16.9%), purplish soil (14.5%) and yellow soil (11.0%). The area has a humid subtropical monsoon climate, featuring distinct seasons with plentiful sunshine, an annual mean temperature of 16.6 °C and abundant precipitation (mean annual precipitation 1,124 mm).

This watershed is one of the branches in the 'Natural Forest Conservation' and 'Conversion of Cropland to Forest' programs funded by the State Forestry Administration, P.R. China. However, high levels of fertilizer and manure usages for perennial crop production in this watershed have increased surface and ground water pollution due to inputs of sediment and nutrients (Shen et al., 2012c). The local government began periodic monitoring of nutrients in the Wu xi station (Figure 1) in 2000, which developed into a regular monitoring program with approximately monthly sampling since 2004. We previously conducted studies on model parameter uncertainty (Shen et al., 2008; Gong et al., 2011; Shen et al., 2012c) and spatial rainfall variability (Shen et al., 2012a) in this region, and we extend these studies further in the present paper to evaluate the impact of rainfall measurement errors on NPS models.

2.2. Preparation of SWAT

In this study, the SWAT model, developed by the Agriculture Research Service of the United States Department of Agriculture (USDA-ARS), was used to quantify the impact of precipitation input on flow, sediment and agricultural chemical yields. The SWAT model is a physically based, semi-distributed model that simulates all the key processes of surface runoff and sediment and nutrient transport (Gassman, 2007). The major components of SWAT include weather, hydrology, erosion, the fates of nutrients and pesticide, agricultural management, and channel processes (Douglas-Mankin et al., 2010). The hydrology component is based on the water balance equation, and the processes of surface and subsurface runoff, percolation, evapotranspiration, and channel transmission losses are simulated. The runoff volume is estimated by the modified SCS curve number method, while the sediment yield is estimated by the modified soil loss equation (MUSLE). A simplification of the EPIC model is used for crop simulation and the description of the nitrogen (N) and phosphorus (P) cycles includes mineralization, nitrification, volatilization and plant uptake. Runoff, sediments, and chemicals are simulated for each hydrologic response unit (HRU) and routed to the river channel. The nutrient transformation in streams is based on the QUAL2E model (Brown and Barnwell, 1987), which integrates nutrient interaction, algae production, and benthic oxygen demand.

In this study, the major GIS input files (obtained from the Chinese Academy of Sciences) for the SWAT model were the digital elevation model (DEM) (at a scale of 1:50,000), land use and land cover map (at a scale of 1:100,000), and soil map (at a scale of 1:1,000,000). The watershed was delineated into 22 sub-basins based on the DEM and specification of streams and inlets/outlets. The sub-basins were portioned into HRUs by setting 0% thresholds of land use, soil type and slope to accurately capture even small areas. An HRU is the lumped area with threshold percentages of land use, management and soil type in a sub-basin (Arnold et al. 1998). Most of the equations in SWAT are solved on the HRU scale. Weather data (daily precipitation, minimum and maximum temperature, solar radiation, and wind speed) were obtained from ten state weather stations located approximately within the watershed. Other weather variables (relative humidity) needed by the model were estimated using the weather generator built into the SWAT model. The pasture management information was collected from Wuxi County, and the timing of manure and fertilizer application, grazing intensity, and dates were obtained from detailed interviews with local farmers. The calculated fertilizer and manure, as well as grazing periods, were built into the management files as SWAT input.

Sensitivity analysis was performed to identify which parameters most influence the outputs of interest. Based on the

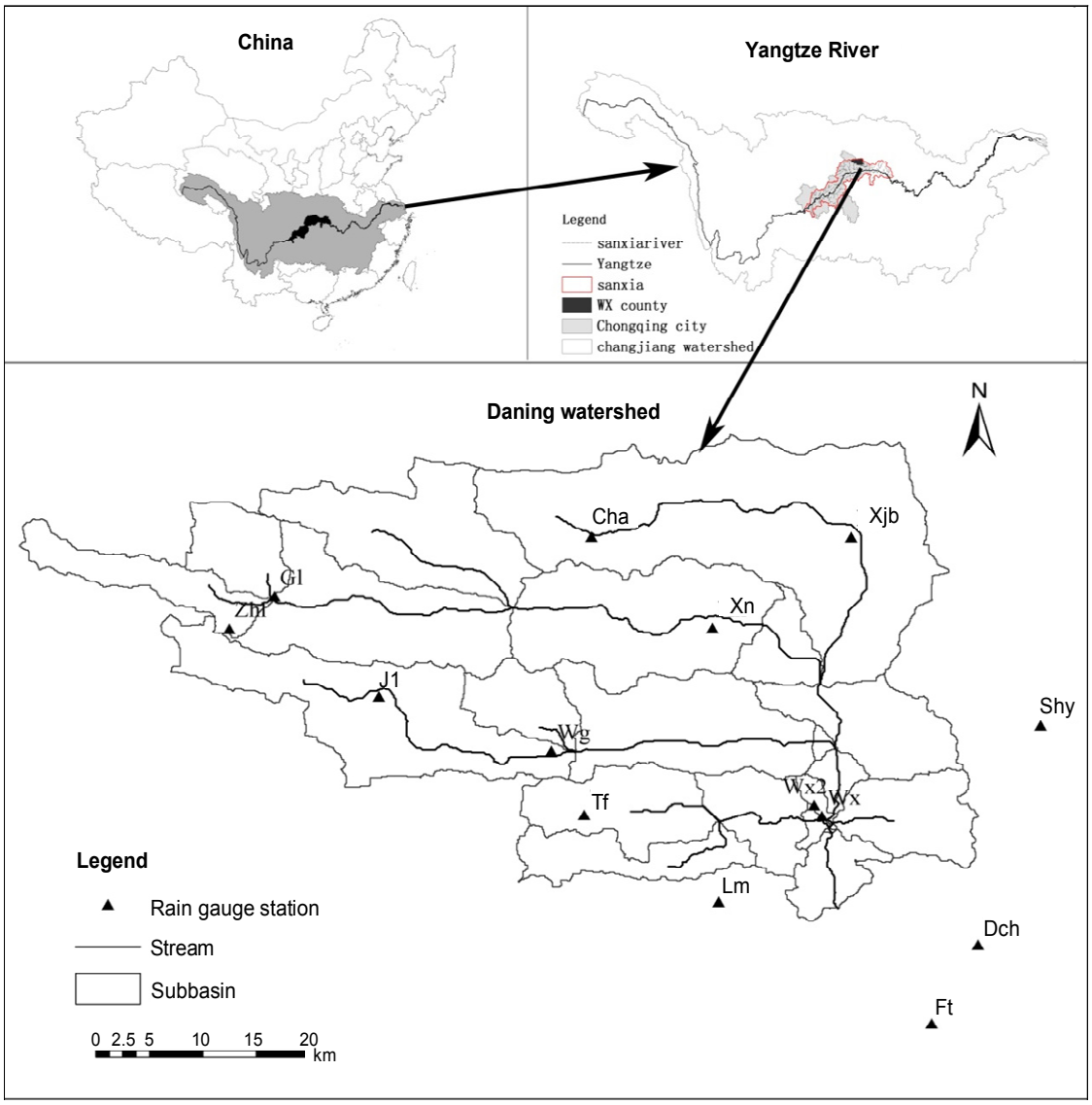

Figure 1. Location of Daning River Watershed.

sensitivity analysis results, 43 parameters were modified for calibrating flow, sediment, and N and P using the monthly measured data collected at the Wuxi station from 2000 to 2007. In this study, parameter calibration and validation were performed using SWATcup (Abbaspour, 2007) based on the monthly step. Calibration was performed from January 2004 to December 2007, and the period of January 2000 to December 2003 was used for validation. The Nash-Sutcliffe coefficients (E_{NS}) for the calibration and validation periods were 0.94 and 0.78 for flow, 0.80 and 0.70 for sediment, and 0.76 and 0.51 for total phosphorous (TP), respectively. To provide a static state instead of subjective personal judgment, the performance ratings typically applied to the E_{NS} by Arabi et al. (2007) were adopted: very good (0.75 ~ 1), good (0.65 ~ 0.75), satisfactory (0.50 ~ 0.65), and unsatisfactory (≤ 0.5). Therefore, the SWAT model was judged to be 'very good' for flow, sediment and TP predictions. More details on the parameter calibration and validation are available in Shen et al. (2012b).

2.3. MC Sampling

In this study, rainfall measurement errors were treated as input uncertainty by the stochastic perturbation approach. The MC method was used because it is a simple concept and very useful for resolving uncertainty issues in complex models (Qin et al., 2008). MC theory is based on the combination of a number of perturbations in the recorded daily rain data, each having a distinct statistical distribution (Rauch et al., 1998; Li et al., 2010; Shen et al., 2012c). In this study, the MC sampling consisted of three steps as described below.

Step 1: Definition of the PDF for rain measurement error.

Here, the rainfall input uncertainty was estimated using the probability of sampling from the range of measurement error. A survey conducted by the State Meteorological Administration (SMA) revealed that the error ranges in rainfall measurements in China varied from ± 4.34% to ± 15.2%, with an average deviation of ± 6.52% (Ren et al., 2003). These data were based on a statistical analysis of the recorded rainfall data from 30 national stations. First, these error data were used to define the sampling range of the rainfall input. Second, the samples were chosen from a normal distribution with a probability distribution function (PDF) given by $X \sim N(\mu, \sigma^2)$, where μ was defined as the initial recorded data and σ as the standard deviation (SD). To cover 99.7% of the values from the error range, the sampling range was designated as (μ − μ × 15.2%, μ + μ × 15.2%). For comparison, we also ran a simulation with a uniform distribution in which all values in the error range were equally sampled.

Step 2: Data sampling.

In the second step, the error range was divided into non-overlapping intervals to cover all measurement values. Because there was no correlation between the daily rainfall data, it was assumed that the recorded data were mutually independent (Li et al., 2009). The recorded daily rain data (2000 ~ 2007) were collected at ten rainfall gauges inside the watershed and nine gauges at sites approximately 30 km outside the watershed boundary. The Co-kriging method was used to generate the spatial rainfall distribution and the generated data were incorporated into the SWAT simulation by creating a virtual rain gauge within the centroid of each sub-watershed. More details could be found in Shen et al. (2012a). Latin hypercube sampling (LHS), developed by Sandia National Laboratories (McKay et al., 1979), employs a constrained sampling scheme instead of random sampling. It is reported that LHS can reduce sampling times and provide 10-fold greater computing efficiency (Vachaud and Chen, 2002). Therefore, the LHS technique was used here. The estimated sample size was based on a statistical analysis of the convergence of the mean value (MV), median value, standard diversion (SD), variance, and coefficient of variation (CV). However, as there were as many as 2922 recorded daily data points, a VBA program was developed to address the batch process of sampling, which can be downloaded from http://iwm.bnu.edu.cn/index_en.php.

Step 3: Model simulation and data analysis.

In the third step, the SWAT model performed a series of simulations based on sample size. The sub-intervals of each daily rainfall value were randomly permutated from a probability distribution over the domain to generate inputs, and every combination of sub-intervals was used as rainfall input for the SWAT model. However, because the SWAT model and the sampling process were in different interfaces, all the model simulations were calculated manually. Thus, the initial daily rain data from multiple rain gauges were considered as the model input, and only the recorded data at the XN gauge were perturbed and sampled. The XN rain gauge was selected because it was closest to the assessment point at which the model parameters were evaluated and would have an obvious impact on the model performance in terms of E_{NS} value. The complete task took almost 30 days on a Centrino Duo processor running at 2.8 GHz. Second, the effect of rainfall uncertainty on the H/NPS model was assessed by quantifying and analyzing the SWAT outputs. The outputs considered were simulated flow, sediment transport, total P (TP), organic N, and dissolved N at the watershed outlet. The corresponding evaluation criteria were the 90% confidence interval (90CI), SD, and CV.

$$\overline{X} = \frac{1}{n}\sum_{i=1}^{n} x_i \tag{1}$$

$$SD = \sqrt{\frac{1}{\mathrm{n}}\sum_{i=1}^{n}\left(x_i - \overline{X}\right)^2} \tag{2}$$

$$CV = \frac{\mathrm{SD}}{\overline{X}} \tag{3}$$

where X_i is the model output, i is the simulation time step, and n is the total number of simulations.

3. Results

3.1. Effect on Rainfall Input Variability

In this section, the selection of sample size was based on a statistical analysis of model outputs. Three sample sizes, 50, 100, and 150, were tested. As shown in Table 1, the MV, SD, variance and CV gradually stabilized as the sample size increased from 50 to 150. In other words, the outputs of flow, sediment load, TP, org N, and dissolved N showed no obvious change when the sample size continued to increase beyond 150. Thus, the following analysis and comparisons are based on a sample size of 150.

The characteristics of the rainfall inputs are then summarized and analyzed in Table 2. A remarkable temporal variability in MV can be observed from 2000 to 2007, varying from 812 mm (2001) to 1537 mm (2003) (a difference of 725.0 mm). The values of SD and CV varied from 6.71 mm (2001) to 13.16 mm (2005) and from 0.007 (2002) to 0.010 (2006), respectively. Further analysis indicated that the CV with monthly input ranged from 0.014 to 0.051, indicating that rainfall measurement errors introduce greater uncertainty when using monthly data input. The averaged values of CV were 0.035 in January, 0.024 in April and 0.022 in July. The CV value was therefore greatest in the low-flow period and the medium-flow period, followed by the high-flow period. This might be explained by the fact that light rainfall may evaporate in the collector as well as that rain gauge response to snow is problematic, as those have to melt to trigger the signal. The

Table 1. The Sample Size and Convergence Rate

Variable	Value	Samples	MV	SD	Variance	CV
Flow (m^3/s)	45.26	50	45.25	0.26	0.07	0.005
		100	45.28	0.25	0.06	0.006
		150	45.29	0.24	0.06	0.006
Sediment (10^3 t)	1903.04	50	1909.14	35.90	1288.81	0.019
		100	1914.13	34.37	1181.64	0.018
		150	1917.00	34.52	1191.63	0.018
TP (t)	156.25	50	156.06	7.20	51.78	0.046
		100	156.36	6.47	41.88	0.041
		150	156.93	6.50	42.20	0.041
Org N (t)	769.88	50	771.68	21.01	441.53	0.027
		100	773.27	19.50	380.16	0.025
		150	775.14	19.32	373.15	0.025
Dissolved N (t)	2648.49	50	2646.29	35.59	1266.74	0.013
		100	2650.40	32.67	1067.55	0.012
		150	2654.67	32.62	1063.91	0.012

Table 2. The Cumulative Precipitation Associated with Measurement Error

Time	Measured data (mm)	MV (mm)	SD (mm)	Variation	CV
2000	1107.4	1107.8	10.81	116.77	0.010
2001	813.0	812.1	6.71	44.98	0.008
2002	1032.1	1033.2	7.55	57.03	0.007
2003	1536.0	1537.7	11.95	142.88	0.008
2004	1124.5	1125.1	10.87	118.15	0.010
2005	1456.5	1454.3	13.16	173.20	0.009
2006	998.5	998.3	9.63	92.73	0.010
2007	1475.0	1475.3	12.93	167.30	0.009

details of the sampled monthly data are provided in Tables 3 to 5.

3.2 Effects on H/NPS Modeling at the Annual Time Steps

This section focuses on error propagation from rainfall uncertainty to H/NPS predictions. The model outputs of annual flow, sediment, TP, org N and dissolved N are illustrated in Figure 2, where the cross line and bars show the MV and CV, respectively. The 90CI, illustrated by the vertical columns in Figure 2, was derived by ordering the 150 sets of outputs and then identifying the 5 and 95% threshold values. The highest levels of flow, sediment load, TP, org N, and dissolved N occurred in 2003: 66.34 m^3/s, 2915.7×10^3 ton, 441.2 ton, 1745.2 ton and 4408.7 ton, respectively. The lowest amounts occurred in 2001: 26.2 m^3/s, 483.1×10^3 ton, 73.2 ton, 186.8 ton and 1492.8 ton. These results can be explained by the rainfall totals, which were highest in 2003 and lowest in 2001 (Table 2), showing a clear relationship between the rainfall totals and the average values of the outputs. This result indicated that rainfall was one of the most important inputs that drive runoff production and mass transport for the H/NPS models. As shown in Figure 2, the CV ranges were 0.012 to 0.016 for flow, 0.034 to 0.058 for sediment load, 0.086 to 0.143 for TP, 0.083 to 0.096 for org N, and 0.037 to 0.087 for dissolved N, with average values of 0.014, 0.043, 0.103, 0.053 and 0.086, respectively. The P and N outputs were more sensitive to rainfall measurement error than predicted flow and sediment. This result indicated that rainfall measurement error would have a varying effect on the modeled variables due to the mechanism of the H/NPS models. It could therefore be concluded that rainfall measurement error is transformed into hydrologic modeling uncertainty and further propagates into even greater NPS modeling uncertainty.

Figure 2 also illustrates the temporal variability of 90CI. The annual 90CI of flow from 2000 to 2007 was 40.11 ~ 44.16, 20.50 ~ 27.35, 30.05 ~ 40.14, 64.80 ~ 68.73, 42.06 ~ 46. 33, 59.71 ~ 64.47, 38.25 ~ 41.50, and 62.49 ~ 67.47 m^3/s, respectively. The width of 90CI in 2003 was 3 times greater than that in 2006, which can be explained by the data in Table 2, showing a close relationship between the amount of the rainfall and the width of 90CI. It was also obvious from Table 2 and the error bars in Figure 2 that the greatest uncertainties in the sediment load, TP, org N, and dissolved N were observed in 2003. The widest 90CI values were 6, 12, 15, and 3 times than the narrowest 90CI for sediment load, TP, org N, and dissolved N, respectively, indicating greater uncertainty in wet years.

Table 3. Statistic Results of Simulated Uncertainty in the Low River Flow Period (January)

Time	Precipitation		Flow		Sediment		TP		Org N		Dissolved N	
	μ (mm)	CV	μ (m^3/s)	CV	μ (10^3 t)	CV	μ (t)	CV	μ (t)	CV	μ (t)	CV
2000	0.60	0.051	2.17	0.003	0.24	0.004	2.07	0.146	0.21	0.145	40.04	0.033
2001	20.40	0.031	9.26	0.036	6.44	0.114	4.82	0.007	3.31	0.197	70.59	0.025
2002	5.80	0.031	1.48	0.033	0.14	0.062	2.67	0.063	0.25	0.063	16.48	0.024
2003	3.50	0.039	1.26	0.040	0.09	0.061	3.11	0.101	0.31	0.107	10.54	0.043
2004	5.50	0.030	5.79	0.052	1.04	0.083	1.58	0.059	0.17	0.067	32.19	0.049
2005	7.50	0.038	3.78	0.029	1.03	0.132	4.57	0.089	1.06	0.200	32.91	0.026
2006	5.50	0.028	0.73	0.042	0.10	0.072	0.91	0.116	0.08	0.120	10.45	0.035
2007	9.50	0.031	5.20	0.036	1.14	0.062	6.99	0.016	0.73	0.014	44.38	0.032
Average	7.29	0.035	3.71	0.034	1.28	0.074	3.34	0.075	0.76	0.114	32.20	0.033

Table 4. Statistic Results of Simulated Uncertainty in the Normal River Flow Period (April)

Time	Precipitation		Flow		Sediment		TP		Org N		Dissolved N	
	μ (mm)	CV	μ (m^3/s)	CV	μ (10^3 t)	CV	μ (t)	CV	μ (t)	CV	μ (t)	CV
2000	19.00	0.024	3.08	0.034	0.45	0.057	2.22	0.078	0.15	0.076	58.26	0.013
2001	63.40	0.026	17.86	0.047	34.61	0.143	6.63	0.145	24.49	0.209	126.24	0.053
2002	141.60	0.019	29.41	0.037	86.45	0.070	20.83	0.105	126.60	0.099	214.32	0.061
2003	122.00	0.023	81.71	0.022	172.70	0.051	32.15	0.076	138.80	0.078	450.69	0.035
2004	36.00	0.025	8.43	0.027	2.98	0.072	3.32	0.039	0.48	0.119	102.46	0.084
2005	132.50	0.028	27.93	0.053	99.11	0.126	20.96	0.273	76.82	0.199	224.56	0.117
2006	188.00	0.024	86.48	0.036	268.00	0.081	69.59	0.154	281.50	0.127	584.92	0.090
2007	119.00	0.021	46.87	0.033	134.50	0.077	20.97	0.099	86.24	0.089	194.65	0.067
Average	102.69	0.024	37.72	0.036	99.85	0.085	22.08	0.121	91.89	0.125	244.51	0.065

Table 5. Statistic Results of Simulated Uncertainty in the High River Flow Period (July)

Time	Precipitation		Flow		Sediment		TP		Org N		Dissolved N	
	μ (mm)	CV	μ (m^3/s)	CV	μ (10^3 t)	CV	μ (mm)	CV	μ (m^3/s)	CV	μ (10^3 t)	CV
2000	339.80	0.023	210.20	0.027	1434.00	0.071	45.55	0.059	744.50	0.055	1846.10	0.056
2001	198.40	0.021	59.33	0.035	133.50	0.074	4.92	0.080	40.93	0.094	379.91	0.040
2002	28.60	0.026	19.88	0.036	8.07	0.061	3.86	0.073	0.39	0.043	156.03	0.077
2003	243.50	0.022	154.30	0.026	722.00	0.077	24.11	0.071	160.90	0.084	811.68	0.038
2004	324.50	0.022	135.60	0.037	916.70	0.088	26.37	0.068	195.70	0.087	723.40	0.044
2005	382.50	0.023	182.80	0.053	1093.00	0.126	25.07	0.077	187.80	0.199	792.90	0.051
2006	108.50	0.023	88.31	0.015	128.60	0.054	4.61	0.045	14.18	0.065	508.55	0.038
2007	378.50	0.017	194.40	0.023	973.60	0.057	26.65	0.053	131.10	0.060	694.27	0.049
Average	250.54	0.022	130.60	0.032	676.18	0.076	20.14	0.066	184.44	0.086	739.11	0.049

3.3 Effects on H/NPS Modeling at the Monthly Time Steps

A further concern is the effect of rainfall measurement errors on H/NPS modeling at the monthly time steps. The monthly outputs of a typical hydrological year (2004) are shown in Figure 3. The CV values of monthly flow, sediment load, TP, Org N, and dissolved N were 0.022 ~ 0.051, 0.049 ~ 0.130, 0.018 ~ 0.111, 0.067 ~ 0.179, and 0.029 ~ 0.064, with average values of 0.037, 0.086, 0.062, 0.129, and 0.048, respectively. Based on the results of this study, the SWAT simulation at the monthly time steps generally provided greater uncertainties than those obtained with the annual time step. The widest 90CI was observed in July, with values of 127 ~ 143 m^3/s for flow, 741×10^3 ~ 1180×10^3 ton for sediment, 22 ~ 32 ton for TP, 48 ~ 166 ton for org N and 410 ~ 799 ton for dissolved N.

This paper further illustrated the seasonal variations in model outputs by choosing January, April and July as low-, medium- and high-flow periods, respectively. As shown in Tables 3 to 5, the average CV values in the low-flow period were 0.034, 0.074, 0.075, 0.114, and 0.033 for flow, sediment load, TP, org N and dissolved N, respectively. The corresponding CV values were 0.036, 0.085, 0.121, 0.125, and 0.065 in the median-flow period and 0.032, 0.076, 0.066, 0.086, and 0.049 in the high-flow period. Tables 3 to 5 further showed that the average SD values of the flow outputs were 0.13, 1.28 and 3.11 m^3/s in the low-, medium- and high-flow periods, respectively. The average SD values were 0.13×10^3,

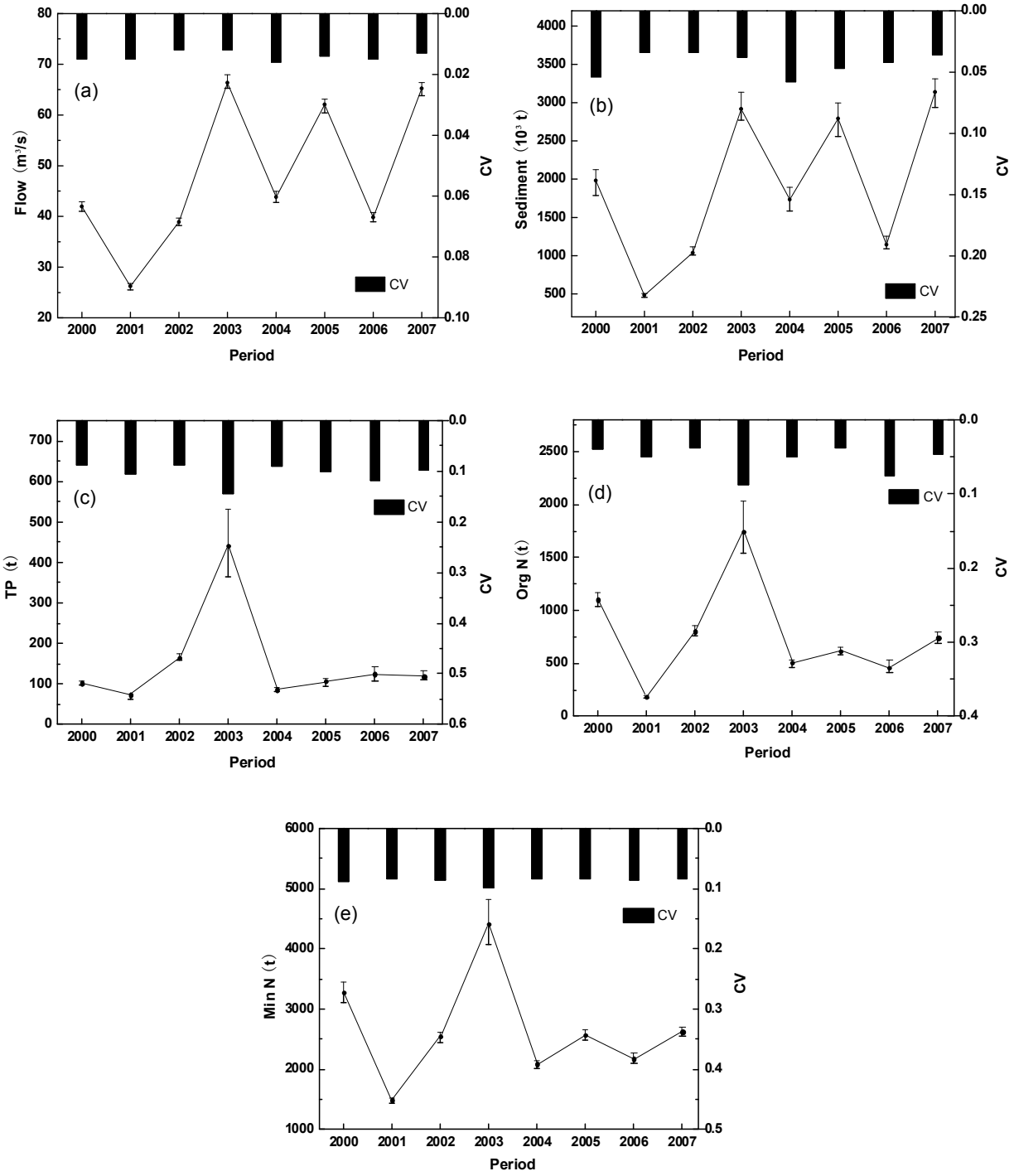

Figure 2. The statistics of annual outputs due to normal distribution.

8.09×10^3, and 40.60×10^3 ton for sediment load; 0.19 ton, 3.05 ton, and 1.31 ton for TP; 0.114 ton, 11.01 ton, and 12.25 ton for org N; and 1.02, 17.15, and 35.86 ton for dissolved N. There was a clear relationship between the amount of rainfall and the width of 90CI, indicating greater uncertainty during high-flow conditions.

4. Discussion

4.1. Effects on Different Variables and Flow Events

As mentioned above, the measurement error in rainfall input propagates through the H/NPS model to the hydrological modeling and, to larger extent, to the NPS simulation.

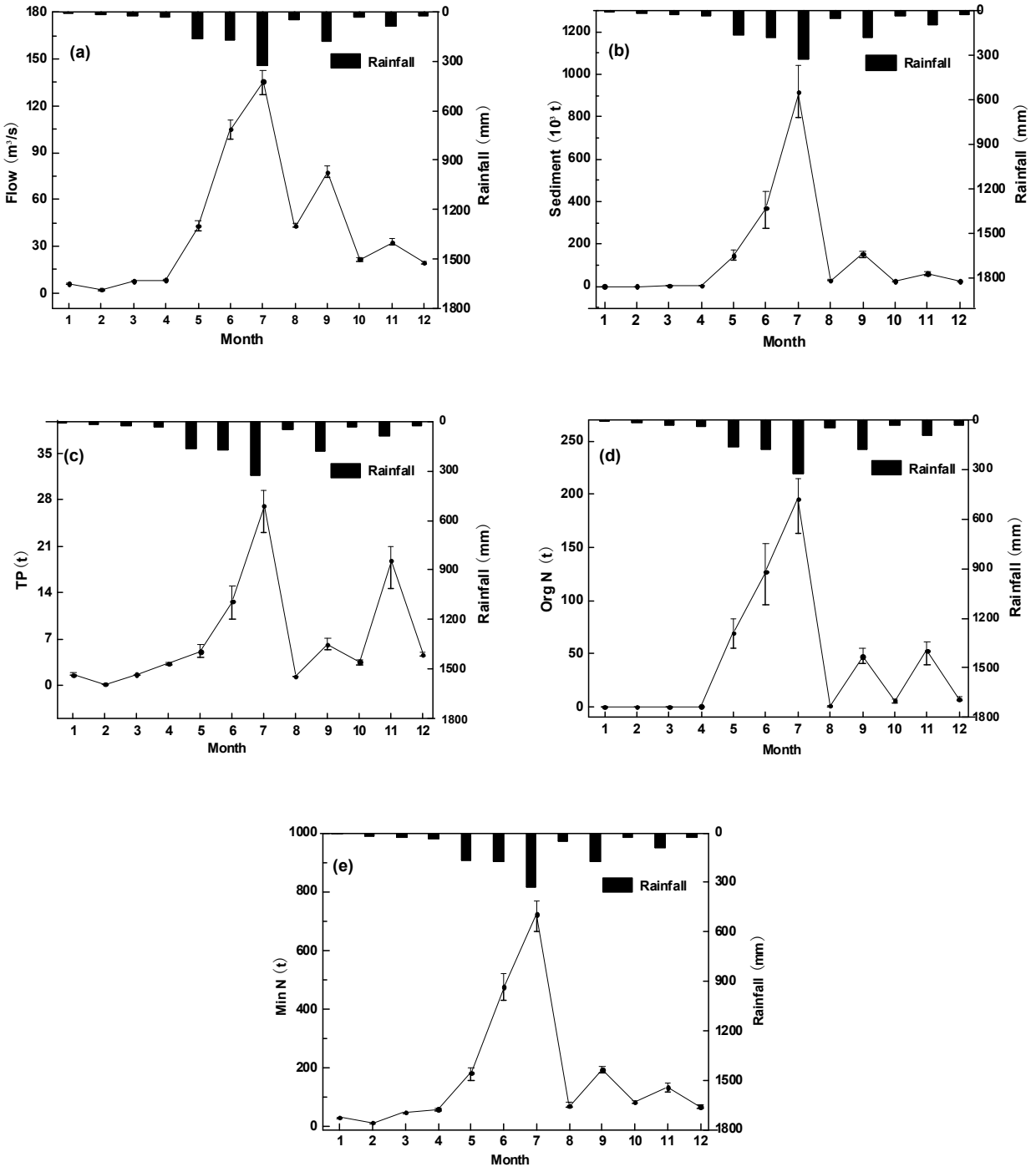

Figure 3. The statistics of monthly outputs due to normal distribution.

Figure 2 highlights the importance of considering measurement errors when calculating P and N at the annual time steps. Figure 3 further demonstrates that the sediment and NPS outputs at the monthly time steps have greater uncertainties. This different behavior of output variables can be explained via the processes of runoff production and mass transport of the H/N-PS models (Cho et al., 2009; Beven et al., 2012). The NPS pollution is not only driven by runoff and soil erosion processes (Karr and Schlosser, 1978) but also affected by other human factors, such as agricultural activities and land use changes (Loague et al., 1998). To better present our study results, the authors define this phenomenon as the 'carry-magnify' effect.

Tables 3 to 5 address the application of uncertainty analysis related to rainfall measurement errors during the high-flow period. In some aspects, the results in these tables are consistent with those of Gong et al. (2011) and Shen et al. (2012b),

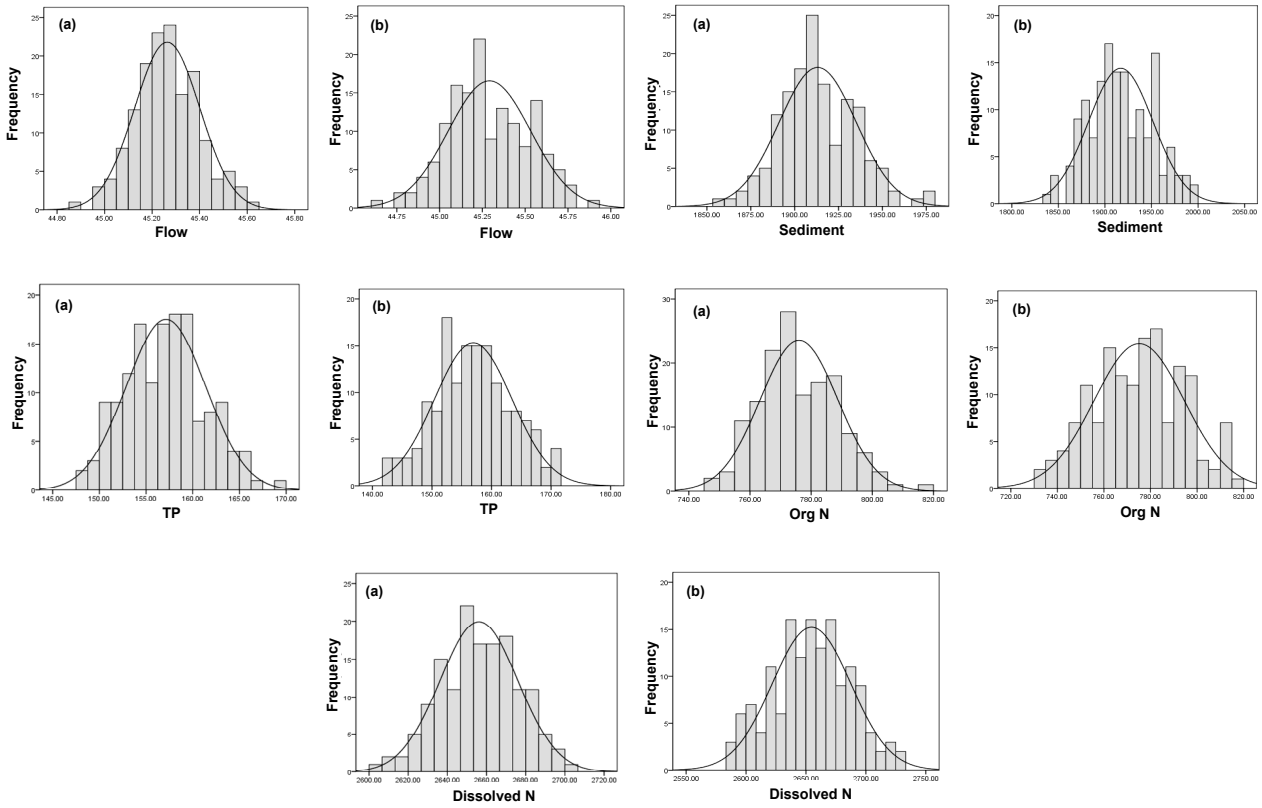

Figure 4. The PDF of outputs due to rainfall measurement error. (a) Uniform pdf; (b) Normal pdf.

who indicated that there would be greater uncertainty during the high-flow conditions. The TGRA is characterized by a tropical monsoon climate with a mean precipitation of 1124 mm and highly variable daily rainfall in the wet season (from June to September) (Shen et al., 2012b; Shen et al., 2012c). Rainfall events occur with irregular duration and magnitude in the wet season (Ouyang et al., 2007; Wu et al., 2012). Therefore, the rain gauge is known to underestimate heavy precipitation, not only because the collection area is relatively small but also because water can accumulate into the collector faster that the buckets are capable of draining it. Therefore, it could be expected that the rainfall measurement error would introduce considerable prediction uncertainty in conjunction with the effects of model parameter, especially during high-flow periods.

4.2. Influence of Error Distribution Type

The above analysis was based on the assumption that the rainfall measurement errors are normally distributed. In previous papers (Bárdossy and Das, 2008; Bohnenstengel et al., 2011; Sun et al., 2012), the suitable distributions of rainfall measurement errors can be expressed by one of the followings: 1) a CI, which is derived by ordering the potential values and later identifying a range of values that act as good estimates of the unknown data sets; 2) databased frequency analysis, designed for each data set using statistical estimation of the PDFs that capture the true data sets. However, the process of specification of the range and associated real distributions for the rainfall measurement errors is a difficult and subjective task due to our imprecise knowledge or insufficient data (Beven and Alcock, 2012). Therefore, it is often assumed that the measurement errors were identically chosen from uniform or normal distribution spanning the feasible range due to their simplicity. In this section, these two commonly used distributions were selected to quantify the impact of error distribution type on the model outputs.

The frequency distributions of outputs were first analyzed using a histogram (Figure 4). The output distributions were investigated by the Shapiro-Wilk method. As the P values were less than 0.05, it could be concluded that the outputs were all normally distributed. For a normal PDF, the ranges of outputs were 44.65 ~ 45.78 m^3/s for flow, 1833.40×10^3 ~ 1998.71×10^3 ton for sediment, 142.14 ~ 171.28 ton for TP, 732.67 ~ 817.21 ton for org N, and 2581.83 ~ 2728.29 ton for dissolved N; meanwhile, for the uniform PDF, the corresponding values were 44.83 ~ 45.61 m^3/s, 1859.45×10^3 ~ 1977.36×10^3 ton, 147.87 ~ 169.84 ton, 745.84 ~ 816.37 ton, and 2604.15 ~ 2706.64 ton, respectively. Additionally, the averaged CV values and the width of 90CI obtained with the normal PDF were 175, 157, 152, 152, and 163% and 170, 153, 164, 170, and 170% of those obtained with the uniform PDF for flow, sediment load, TP, org N and dissolved N, respectively. This behavior might be explained by the shape of the normal sam-

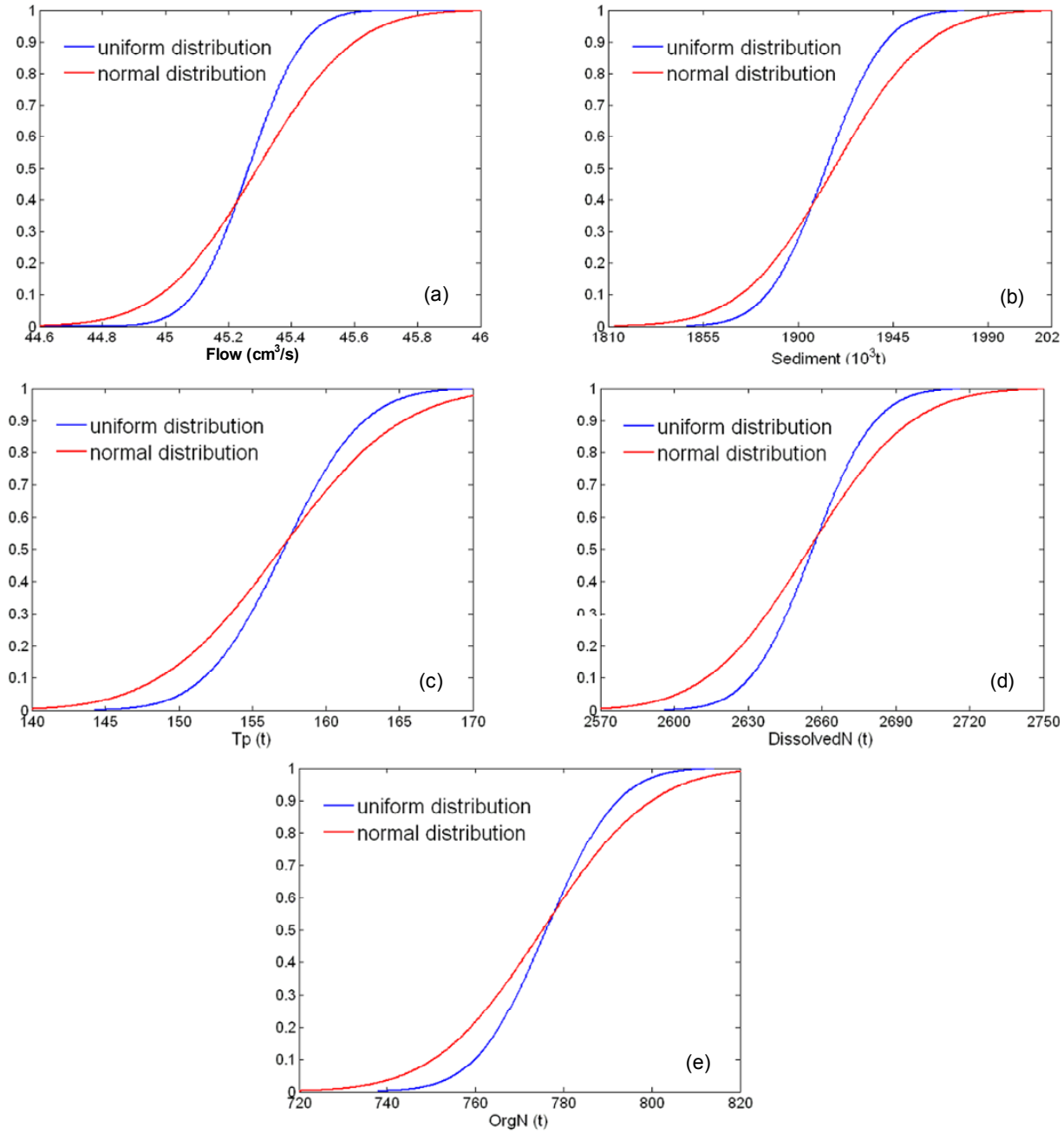

Figure 5. The CDF of outputs due to normal and uniform PDF.

ple distribution, which contains more samples near the initial recorded rainfall data and fewer towards the upper and lower limits (Li et al., 2010; Shen et al., 2012c); therefore, sampling from these data regions would create a better likelihood of achieving good results. Therefore, in the case of this study, a normal PDF improved H/NPS prediction accuracy at the expense of a wider 90CI. Based on this study, the selection of PDF might involve a trade-off between modeling precision and prediction uncertainty.

The cumulative distribution functions (CDFs) are plotted in Figure 5. Specific values were identified as levels (thresholds) beyond which rapid acceleration or deceleration of the cumulative distribution of outputs occurred. Such threshold values for flow, sediment load, TP, org N and dissolved N were 45.23 m^3/s, 1906×10^3, 157, 777, and 2648 ton in the TGRA, respectively. This result suggests that once the measurement error exceeded a critical value, the H/NPS outputs responded differently depending on whether a normal or uni-

form PDF was applied. It was found that the CDFs of the model outputs did not behave linearly due to the nonlinear model structure among the parameters. It has been common to adopt different types of distributions, such as uniform, gamma and log-normal distributions, to describe the differences between the original and perturbed errors (Li et al., 2010; Shen et al., 2012c). The results highlighted the importance of considering PDF for model inputs during the hydrological and NPS modeling process; hence, a user should determine the PDF of the rainfall input corresponded to the equipment characteristics or based on the data-based frequency analysis.

4.3. Exportation of This Study

These results obtained from this study can only be extrapolated to other models or sites with caution. In the TGRR, rain gauges are still the majority of the instrumentation available for watershed models because they are relatively cheap and easy to install and calibrate (Tapiador et al., 2012). The most common rain gauges in this region are the mechanical instrument, typically consisting of a collecting area and a signal system (Ren et al., 2003; Tapiador et al., 2012). More advanced techniques, such as radar data, may also be used to provide better spatial rainfall distributions than rain gauge measurements. However, radar data are also subject to various errors such as errors in reflectivity-rainfall (Z-R) relationships, variation in the vertical profile of reflectivity, and spatial and temporal sampling among others (AghaKouchak et al., 2010). Thus, the rainfall measurement error should be considered as an inherent part of modeling watershed systems (Schuurmans and Bierkens, 2007), resulting in what Beven (2006) called non-ideal cases. In this case, this paper proposed stochastic modeling within the framework of Generalized Likelihood Uncertainty Estimation (GLUE) to find an acceptable fit of behavior models (Guo et al., 2003; Franz and Hogue, 2011; Li et al., 2011; Fan and Huang, 2012).

In the TGRR, those mechanical types of rain gauges are reported to underestimate heavy precipitation because the collection area is relatively small and heavy precipitation is difficult to capture using buckets (Tapiador et al., 2012). They are also problematic for the dry season, as light rainfall may evaporate or otherwise leave from the collector. Many studies have revealed that watershed models underestimate the flow during the wet period and overestimate this variable during the dry season (Renard et al., 2011; Shen et al., 2012c). Considering the inherent source and nature of errors, it was recognized that compensating this error by considering real measurement errors during the wet season and dry season. In addition, the rainfall input errors are usually interpolated and assigned to the center of the model grid box as the model input. For this reason, future progress should depend on establishing dense observational networks in the estimate of rainfall input over the catchment area. More details about this issue can be found in our previous study (Shen et al., 2012a).

5. Conclusions

This paper investigated the effects of rainfall measurement errors on H/NPS models. The SWAT model and the MC technique were combined to quantify the prediction uncertainty in the Daning River watershed in the TGRA of China. Based on the results obtained from this paper, the measurement error in rainfall input propagates through the H/NPS model to the hydrologic modeling and, to larger extent, the NPS simulation. The rainfall measurement error should be considered as a notably important source of uncertainty in H/NPS modeling and uncertainty analysis for SWAT applications should consider the model variables of interest. During high-flow periods, it was expected that rainfall measurement error would introduce considerable prediction uncertainty in conjunction with the effects of the model parameters.

However，the current set-up of the study (single XN rain gauge) is relatively fairly simple approach. The conclusion of this study is site specific and may be different if the rainfall spatial distributions are significantly different from those in the Daning watershed discussed here. Therefore, to provide a scientific basis for the watershed simulation of the TGRA, more tests may be needed to determine whether the ungauged catchment and multi-rain-gauge watersheds could be estimated in this way.

Acknowledgments. The study was supported by the National Science Foundation for Distinguished Young Scholars (No. 5102-5933), the National Science Foundation for Innovative Research Groups (No. 51121003), and the Nonprofit Environment Protection Specific Project (No. 200709024). The authors wish to express their gratitude to the Journal of Environmental Informatics, and to the anonymous reviewers who helped to improve this paper through their thorough review.

References

Abbaspour, K.Y., Maximov, I., Siber, R., Bogner, K., Mieleitner, J., Zobrist, J., and Srinivasan, R. (2007). Modelling hydrology and water quality in the preailpine/alpine Thur watershed using SWAT. *J. Hydrol.,* 333(2-4), 413-430. http://dx.doi.org/10.1016/j.jhydrol.2006.09.014

AghaKouchak, A., Habib, E., and Bardossy, A. (2010). Modeling radar rainfall estimation uncertainties: Random error model. *J. Hydrol. Eng.,* 15(4), 265-274. http://dx.doi.org/10.1061/(ASCE)HE.1943-5584.0000185

Arnold, J.G., Srinivasan, R., Muttiah, R.S., and Williams, J.R. (1998). Large area hydrologic modeling and assessment: Part I. Model development. *J. Am. Water Resour. Assoc.,* 34(1), 73-89. http://dx.doi.org/10.1111/j.1752- 1688.1998.tb05961.x.

Bárdossy, A., and Das, T. (2008). Influence of rainfall observation network on model calibration and application. *Hydrol. Earth Syst. Sci.,* 12(1), 77-89. http://dx.doi.org/10.5194/hess-12-77-2008

Beven, K. (2006). A manifesto for the equifinality thesis. *J. Hydrol.,* 320(1-2), 18-36. http://dx.doi.org/10.1016/j.jhydrol.2005.07.007

Beven, K., Buytaert, W., and Smith, L.A. (2012). On virtual observatories and modelled realities (or why discharge must be treated as a virtual variable). *Hydrol. Process.,* 26(12), 1906-1909.

http://dx.doi.org/10.1002/hyp.9261

Beven, K.J., and Alcock, R.E. (2012). Modelling everything everywhere: A new approach to decision-making for water management under uncertainty. *Freshw. Biol.,* 57, 124-132. http://dx.doi.org/10.1111/j.1365-2427.2011.02592.x

Bohnenstengel, S.I., Schluenzen, K.H., and Beyrich, F. (2011). Representativity of in situ precipitation measurements - A case study for the LITFASS area in North-Eastern Germany. *J. Hydrol.,* 400(3-4), 387-395. http://dx.doi.org/10.1016/j.jhydrol.2011.01.052

Brown, L.C., and Barnwell, T.O. (1987). The Enhanced stream water quality models QUAL2E and QUAL2E-UNCAS: Documentation and user manual. E.R.L. USEPA. Athens.

Cho, J., Bosch, D., Lowrance, R., Strickland, T., and Vellidis, G. (2009). Effect of spatial distribution of rainfall on temporal and spatial uncertainty of SWAT output. *Trans. ASAE,* 52(5), 1545-1555. http://dx.doi.org/10.13031/2013.29143

Douglas-Mankin, K.R., Srinivasan, R., and Arnold, J.G. (2010). Soil and Water Assessment Tool (SWAT) model: Current developments and applications. *Trans. ASABE,* 53(5), 1423-1431. http://dx.doi.org/10.13031/2013.34915

Fan, Y.R., and Huang, G.H. (2012). A robust two-step method for solving interval linear programming problems within an environmental management context. *J. Environ. Inf.,* 19(1), 1-9. Http://dx.doi.org/10.3808/jei.201200203

Faurès, J.M., Goodrich, D.C., Woolhiser, D.A., and Sorooshian, S. (1995). Impact of small-scale spatial rainfall variability on runoff modeling. *J. Hydrol.,* 173(1-4), 309-326. http://dx.doi.org/10.1016/0022-1694(95)02704-S

Faures, J.M., Goodrich, D.C., Woolhiser, D.A., and Sorooshian, S. (1995). Impact of small-scale spatial rainfall variability on runoff modeling. *J. Hydrol.,* 173(1-4), 309-326. http://dx.doi.org/10.1016/0022-1694(95)02704-S

Franz, K.J., and Hogue, T.S. (2011). Evaluating uncertainty estimates in hydrologic models: Borrowing measures from the forecast verification community. *Hydrol. Earth Syst. Sci.,* 15(11), 3367-3382. http://dx.doi.org/10.5194/hess-15-3367-2011

Fu, S., Sonnenborg, T.O., Jensen, K.H., and He, X. (2011). Impact of precipitation spatial resolution on the hydrological response of an integrated distributed water resources model. *Vadose Zone J.,* 10(1), 25-36. http://dx.doi.org/10.2136/vzj2009.0186

Gabellani, S., Boni, G., Ferraris, L., Vonhardenberg, J., and Provenzale, A. (2007). Propagation of uncertainty from rainfall to runoff: A case study with a stochastic rainfall generator. *Adv. Water Resour.,* 30(10), 2061-2071. http://dx.doi.org/10.1016/j.advwatres.2006.11.015

Gassman, P.W., Green, C.H., and Arnold, J.G. (2007). The Soil and Water Assessment Tool: Historical development, applications, and future research directions. *Trans. ASABE,* 50(4), 1211-1250. http://dx.doi.org/10.13031/2013.23637

Gong, Y., Shen, Z., Hong, Q., Liu, R., and Liao, Q. (2011). Parameter uncertainty analysis in watershed total phosphorus modeling using the GLUE methodology. *Agric., Ecosyst. Environ.,* 142(3-4), 246-255. http://dx.doi.org/10.1016/j.agee. 2011.05.015.

Gunalay, Y., Yeomans, J.S., and Huang, G.H. (2012). Modelling to generate alternative policies in highly uncertain environments: An application to municipal solid waste management planning. *J. Environ. Inf.,* 19(2), 58-69.

Guo, H.C., Liu, L., and Huang, G.H. (2003). A stochastic water quality forecasting system for the Yiluo River. *J. Environ. Inf.,* 1(2), 18-32. http://dx.doi.org/10.3808/jei.200300010

Hughes, D.A. (2010). Hydrological models: Mathematics or science? *Hydrol. Process.,* 24(15), 2199-2201. http://dx.doi.org/10.1002/hyp.7805

Kao, J.J., and Hong, H.J. (1996). NPS model parameter uncertainty analysis for an off-stream reservoir. *Water Resour. Bull.,* 32(5), 1067-1079. http://dx.doi.org/10.1111/j.1752-1688.1996.tb04074.x

Karr, J.R., and Schlosser, I.J. (1978). Water resources and the land-water interface. *Science,* 201(4352), 229-234. http://dx.doi.org/10.1126/science.201.4352.229

Li, Y.P., Huang, G.H., and Sun, W. (2011). Management of uncertain information for environmental systems using a multistage fuzzy-stochastic programming model with soft constraints. *J. Environ. Inf.,* 18(1), 28-37. http://dx.doi.org/10.3808/jei.2011001 96

Li, Z.L., Shao, Q.X., Xu, Z.X., and Cai, X.T. (2010). Analysis of parameter uncertainty in semi-distributed hydrological models using bootstrap method: A case study of SWAT model applied to Yingluoxia watershed in northwest China. *J. Hydrol.,* 385(1-4), 76-83. http://dx.doi.org/10.1016/j.jhydrol.2010.01.025

Li, Z.L., Xu, Z.G., Shao, Q.X., and Yang, J. (2009). Parameter estimation and uncertainty analysis of SWAT model in upper reaches of the Heihe river basin. *Hydrol. Process.,* 23(19), 2744-2753. http://dx.doi.org/10.1002/hyp.7371

Liu, Y., Freer, J., Beven, K., and Matgen, P. (2009). Towards a limits of acceptability approach to the calibration of hydrological models: Extending observation error. *J. Hydrol.,* 367(1-2), 93-103. http://dx.doi.org/10.1016/j.jhydrol.2009.01.016

Loague, K., Corwin, D.L., and Ellsworth, T.R. (1998). The challenge of predicting nonpoint source pollution. *Environ. Sci. Technol.,* 32 (5), 130A-133A. http://dx.doi.org/10.1021/es984037j

McKay, M.D., Conover, W.J., and Beckman, R.J. (1979). A comparison of three methods for selecting values of input variables in the analysis of output from a computer code. *Technometrics,* 21 (2), 239-245.

McMillan, H., Jackson, B., Clark, M., Kavetski, D., and Woods, R. (2011). Rainfall uncertainty in hydrological modelling: An evaluation of multiplicative error models. *J. Hydrol.,* 400(1-2), 83-94. http://dx.doi.org/10.1016/j.jhydrol. 2011.01.026.

Moriasi, D.N., Arnold, J.G., Van Liew, M.W., Bingner, R.L., Harmel, R.D., and Veith, T.L. (2007). Model evaluation guidelines for systematic quantification of accuracy in watershed simulations. *Trans. ASABE,* 50(3), 885-900. http://dx.doi.org/10.13031/2013. 23153

Moulin, L., Gaume, E., and Obled, C. (2009). Uncertainties on mean areal precipitation: Assessment and impact on streamflow simulations. *Hydrol. Earth Syst. Sci.,* 13(2), 99-114. http://dx.doi.org/10.5194/hess-13-99-2009

Osborn, H.B., Renard, K.G., and Simanton, J.R. (1979). Dense networks to measure convective rainfall in the southwestern United States. *Water Resour. Res.,* 15(6), 1701-1711. http://dx.doi.org/10.1029/WR015i006p01701

Ouyang, W., Hao, F.H., Wang, X.L., and Cheng, H.G. (2007). Nonpoint source pollution responses simulation for conversion cropland to forest in mountains by SWAT in China. *Environ. Manage.,* 41(1), 79-89. http://dx.doi.org/10.1007/s00267-007-9028-8

Qin, X.S., Huang, G.H., and Chakma, A. (2008). Modeling groundwater contamination under uncertainty: A factorial-design-based stochastic approach. *J. Environ. Inf.,* 11(1), 11-20. http://dx.doi.org/10.3808/jei.200800106

Ren, Z.H., Wang, G.L., and Zou, F.L. (2003). The research of precipitation measurement errors in China (in chinese). *ACTA Meteo. China,* 64, 621-627.

Renard, B., Kavetski, D., Leblois, E., Thyer, M., Kuczera, G., and Franks, S.W. (2011). Toward a reliable decomposition of predictive uncertainty in hydrological modeling: Characterizing rainfall errors using conditional simulation. *Water Resour. Res.,* 47. http://dx.doi.org/10.1029/2011WR010643

Schuurmans, J.M., and Bierkens, M.F.P. (2007). Effect of spatial distribution of daily rainfall on interior catchment response of a distributed hydrological model. *Hydrol. Earth Syst. Sci.,* 11(2), 677-693.

http://dx.doi.org/10.5194/hess-11-677-2007

Seed, A.W., and Austin, G.L. (1990). Sampling errors for rain gauge-derived mean areal daily and monthly rainfall. *J. Hydrol.,* 118(1-4), 163-173. http://dx.doi.org/10.1016/0022-1694 (90)90256-W

Shen, Z.Y., Chen, L., Liao, Q., Liu, R.M., and Hong, Q. (2012a). Impact of spatial rainfall variability on hydrology and nonpoint source pollution modeling. *J. Hydrol.,* (472-473), 205-215. http://dx.doi.org/10.1016/j.jhydrol.2012.09.019

Shen, Z.Y., Chen, L., and Chen, T. (2012b). Analysis of parameter uncertainty in hydrological and sediment modeling using GLUE method: A case study of SWAT model applied to Three Gorges Reservoir Region, China. *Hydrol. Earth Syst. Sci.,* 16(1), 121-132. http://dx.doi.org/10.5194/hess-16-121-2012

Shen, Z.Y., Chen, L., and Chen, T. (2012c). The influence of parameter distribution uncertainty on hydrological and sediment modeling: A case study of SWAT model applied to the Daning watershed of the Three Gorges Reservoir Region, China. *Stochastic Environ. Res. Risk Assess.,* 27(1), 235-251. http://dx.doi.org/10.1007/s00477-012-0579-8

Shi, Z.H., Ai, L., Fang, N.F., and Zhu, H.D. (2012). Modeling the impacts of integrated small watershed management on soil erosion and sediment delivery: A case study in the Three Gorges Area, China. *J. Hydrol.,* 438-439, 156-167. http://dx.doi.org/10.1016/j.jhydrol.2012.03.016

Sun, W., Ishidaira, H., and Bastola, S. (2012). Prospects for calibrating rainfall-runoff models using satellite observations of river hydraulic variables as surrogates for in situ river discharge measurements. *Hydrol. Process.,* 26(6), 872-882. http://dx.doi.org/10.1002/hyp.8301

Tapiador, F.J., Turk, F.J., Petersen, W., Hou, A.Y., Garcia-Ortega, E., Machado, L.A.T., Angelis, C.F., Salio, P., Kidd, C., Huffman, G.J., and de Castro, M. (2012). Global precipitation measurement: Methods, datasets and applications. *Atmos. Res.,* 104, 70-97. http://dx.doi.org/10.1016/j.atmosres.2011.10.021

Vachaud, G., and Chen, T. (2002). Sensitivity of a large-scale hydrologic model to quality of input data obtained at different scales; distributed versus stochastic non-distributed modeling. *J. Hydrol.,* 264, 101-112. http://dx.doi.org/10.1016/S0022-1694(02) 00069-0

Rauch, W., Thurner, N., and Harremoes, P. (1998). Required accuracy of rainfall data for integrated urban drainage modeling. *Water Sci. Technol.,* 37(11), 81-89. http://dx.doi.org/10.1016/S0273-1223(98) 00319-9

Wu, L., Long, T.Y., Liu, X., and Mmereki, D. (2012). Simulation of soil loss processes based on rainfall runoff and the time factor of governance in the Jialing River Watershed, China. *Environ. Monit. Assess.,* 184, 3731-3748. http://dx.doi.org/10.1007/s10661-01122-20-6

Zhang, Q., and Lou, Z. (2011). The environmental changes and mitigation actions in the Three Gorges Reservoir region, China. *Environ. Sci. & Policy,* 14, 1132-1138. http://dx.doi.org/10.1016/j.envsci.2011.07.008.